FLUTTER INSTABILITY ANALYSIS OF BRIDGE DECKS USING THE STEP-BY-STEP METHOD

Nguyen Van Khang[*]**, Tran Ngoc An**
Hanoi University of Science and Technology, Vietnam
[*]E-mail: khang.nguyenvan2@hust.edu.vn
Received January 13, 2013

Abstract. The branch switch characteristics of coupled flutter are clarified by use of Step-by-Step flutter analysis. In the case of typical coupled flutter instability, the branch switch characteristic from torsional branch to heaving branch is observed. In this paper, a revised step-by-step analysis method is proposed and a calculating program using MATLAB is build. Finally, the flutter behavior of the Cao Lanh Bridge, which is the long bridge in Vietnam, is studied from the point of view of flutter in two-degrees of freedom, namely torsional and heaving motion.

Keywords: Flutter instability, step-by-step analysis, numerical simulation, vibration of bridge.

1. INTRODUCTION

After total collapse of Tacoma Narrow Bridge in USA, 1940 due to the flutter instability, the aerodynamic and aeroelastic phenomena have been focused on bridge structures. Especially, the Flutter instability (known as aeroelastic instability) is closely related to flexible long-span bridges, because it is a reason for structural catastrophe. The bridge aeroelasticity implies for the flutter instability. It tends to be most concern on flexible long-span bridges at high wind velocity in which the aeroelastic interaction between wind and structure generates the so-called self-excited aeroelastic forces. The aeroelastic instability, however, occurs relating to negative damping mechanism due to combination between structural damping and aerodynamic one. Traditionally, two types of the flutter instability have been classified based on characteristics of bridge's modal participation at instability state. Torsional flutter is the case that only torsional mode participates dominantly to such critical state, whereas coupled flutter occurs when two torsional and heaving modes simultaneously involve in.

In only last two decades of the 20th century, many large-span bridges have been successfully built in the world. Further bridges are hinged on super long span and more slender structures as the main tendency of research and development of bridge engineering in the few coming decades. The longer, the more slender structures, however, also face with many difficulties, especially in the dynamic, seismic and aerodynamic behaviors. It

is widely agreed that the long-span bridges are very prone to the aerodynamic effects and the wind-induced vibration. In recent years, a number of long cable-stayed bridges have been built in Vietnam (My Thuan Bridge, Binh Bridge, Bai Chay Bridge, Can Tho Bridge, Han River Bridge, Phu My Bridge, Cao Lanh Bridge, Rachmieu Bridge, ...). Vietnam is a country with a lot of wind and storm. Therefore, it is necessary to investigate the flutter instability of long-span bridges.

Flutter problems can be approximately divided by analytical and experimental methods and simulation techniques. The experimental approach is thanks to free vibration tests on 2D bridge sectional model in wind tunnel laboratory. Computational fluid dynamics (CFD) technique has gained much development so far to become useful supplemental tools beside analytical and experimental methods and it is also predicted broadly that such the CFD might replace wind tunnel tests in future; however, this technique still has many limitations to cope with complexity of bridge sections and nature of 3D bridge structures.

To solve 2DOF heaving-torsional motion equations, there are two powerful analytical methods: so-called the complex eigenvalue method [1, 2] and the step-by-step method [3–8]. 2DOF heaving-torsional motion system has been usually taken the cases of unit structural length subjected to unit self-controlled forces into consideration. The 2DOF heaving-torsional motion systems, moreover, can be known in sectional model tests in wind tunnels.

This paper presents the application of the step-by-step method [3, 6] for calculating the flutter instability of a long cable-stayed bridge, which have been built in Vietnam.

2. STEP-BY-STEP METHOD FOR 2 DOF HAVING-TORSIONAL VIBRATION

The flutter motion equations of 2DOF heaving-torsional system (Fig. 1) can be written as follows

$$m\ddot{h}(t) + c_h\dot{h}(t) + k_h h(t) = L_h \tag{1}$$

$$I\ddot{\alpha}(t) + c_\alpha\dot{\alpha}(t) + k_\alpha\alpha(t) = M_\alpha \tag{2}$$

where: m, c_h, k_h are mass, damping coefficient and stiffness, respectively associated with heaving motion. I, c_α, k_α are mass inertia moment, damping coefficient and stiffness, respectively, associated with torsional motion. L_h, M_α are self-controlled lift and moment.

The self-controlled forces L_h, M_α can be determined by either of Theodorsen's circulation function or Scanlan's flutter derivatives under frequency approach. The Scanlan's self-controlled forces have been applied for the flutter motion equations for various types of cross sections thank to experimentally-determined flutter derivatives.

According to this approach, the self-controlled forces per unit span length can be expressed as

$$L_h = \frac{1}{2}\rho U^2 B\left[KH_1^*(K)\frac{\dot{h}}{U} + KH_2^*(K)\frac{B\dot{\alpha}}{U} + K^2H_3^*(K)\alpha + K^2H_4^*(K)\frac{h}{B}\right] \tag{3}$$
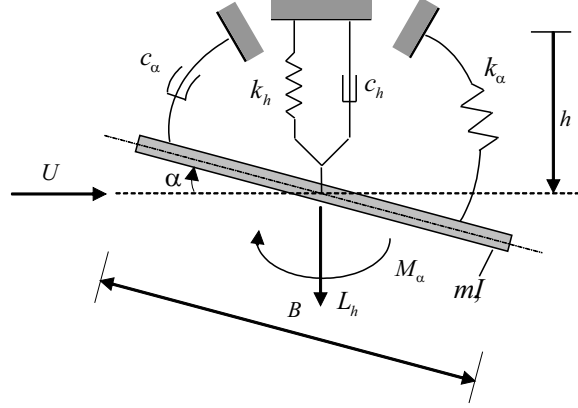
Fig. 1. Mechanical model of the bridge deck

$$M_\alpha = \frac{1}{2}\rho U^2 B^2 \left[KA_1^*(K)\frac{\dot{h}}{U} + KA_2^*(K)\frac{B\dot{\alpha}}{U} + K^2 A_3^*(K)\alpha + K^2 A_4^*(K)\frac{h}{B} \right] \tag{4}$$

where the nondimensional reduced frequency K is defined as

$$K = \frac{B\omega}{U} \tag{5}$$

B is the width of the bridge deck, U is the uniform approach velocity of the wind and ω is the circular frequency of oscillation. The eight real coefficients H_j^* and $A_j^*(j = 1, \ldots, 4)$ are the flutter derivatives based on Scanlans approach.

Above Eqs. (1), (2) can be rewritten in the standard form as follows

$$\ddot{h} + 2\zeta_h\omega_h\dot{h} + \omega_h^2 h = \frac{\rho B^2}{2m}\omega_F H_1^*\dot{h} + \frac{\rho B^2}{2m}\omega_F^2 H_4^* h + \frac{\rho B^3}{2m}\omega_F H_2^*\dot{\alpha} + \frac{\rho B^3}{2m}\omega_F^2 H_3^*\alpha \tag{6}$$

$$\ddot{\alpha} + 2\zeta_\alpha\omega_\alpha\dot{\alpha} + \omega_\alpha^2\alpha = \frac{\rho B^3}{2I}\omega_F A_1^*\dot{h} + \frac{\rho B^3}{2I}\omega_F^2 A_4^* h + \frac{\rho B^4}{2I}\omega_F A_2^*\dot{\alpha} + \frac{\rho B^4}{2I}\omega_F^2 A_3^*\alpha \tag{7}$$

Step 1: In torsional system, harmonic torsional motion is assumed that

$$\alpha = \alpha_0 \sin \omega_F t \tag{8}$$

where α_0 is the amplitude of torsional motion and t is the time.

$$\dot{\alpha} = \alpha_0\omega_F \cos \omega t = \alpha_0\omega_F \sin\left(\omega_F t + \frac{\pi}{2}\right) \tag{9}$$

Step 2: In heaving system, the heaving motion is generated by external forces caused by the torsional motion, as forced vibration:

Substituting Eqs. (8) and (9) into Eq. (6), we have the differential equation of forced heaving vibration

$$\ddot{h} + \left[2\zeta_h\omega_h - \frac{\rho B^2}{2m}\omega H_1^*\right]\dot{h} + \left[\omega_h^2 - \frac{\rho B^2}{2m}\omega_F^2 H_4^*\right] h = \frac{\rho B^3}{2m}\omega_F H_2^*\dot{\alpha} + \frac{\rho B^3}{2m}\omega_F^2 H_3^*\alpha$$
$$= \frac{\rho B^3}{2m}\omega_F H_2^*\alpha_0\omega_F \sin\left(\omega_F t + \frac{\pi}{2}\right) + \frac{\rho B^3}{2m}\omega_F^2 H_3^*\alpha_0 \sin \omega_F t \tag{10}$$

Rewriting Eq. (10) in the standard form

$$\ddot{h} + 2\zeta_h^* \omega_h^* \dot{h} + \omega_h^{*2} h = \frac{\rho B^3}{2m} H_2^* \alpha_0 \omega_F^2 \sin\left(\omega_F t + \frac{\pi}{2}\right) + \frac{\rho B^3}{2m} \omega_F^2 H_3^* \alpha_0 \sin \omega_F t \tag{11}$$

where

$$\omega_h^{*2} = \omega_h^2 - \frac{\rho B^2}{2m} \omega_F^2 H_4^* \tag{12}$$

$$\zeta_h^* = \left[2\zeta_h \omega_h - \frac{\rho B^2 \omega_F}{2m} H_1^*\right] / (2\omega_h^*) \tag{13}$$

Solution of Eq. (11) consists of the following components

$$h = \bar{h} + h_1 + h_2 \tag{14}$$

(i) $\bar{h}$ is the total solution of free vibration equation

$$\ddot{h} + 2\zeta_h^* \omega_h^* \dot{h} + \omega_h^{*2} h = 0 \tag{15}$$

which takes a form

$$h = h_0 e^{-\zeta_h^* t} \sin\left(\omega_h^* t - \phi\right) \tag{16}$$

 Note that for large values of t, the homogeneous solution (16) approaches zero and the total solution of Eq. (11) approaches the particular solution [9].

(ii) h_1 is the solution of forced vibration equation

$$\ddot{h} + 2\zeta_h^* \omega_h^* \dot{h} + \omega_h^{*2} h = \frac{\rho B^3}{2m} H_2^* \alpha_0 \omega_F^2 \sin\left(\omega_F t + \frac{\pi}{2}\right) \tag{17}$$

It takes a form

$$h_1 = h_{10} \sin\left(\omega_F t + \frac{\pi}{2} - \theta\right) \tag{18}$$

where

$$h_{10} = \frac{\frac{\rho B^3}{2m} |H_2^*| \alpha_0 \omega_F^2}{\sqrt{\left(\omega_h^{*2} - \omega_F^2\right)^2 + 4\zeta_h^{*2} \omega_h^{*2} \omega_F^2}} \tag{19}$$

$$\sin\theta = \frac{2\zeta_h^* \omega_h^* \omega_F H_2^*}{|H_2^*| \sqrt{\left(\omega_h^{*2} - \omega_F^2\right)^2 + 4\zeta_h^{*2} \omega_h^{*2} \omega_F^2}},$$

$$\cos\theta = \frac{\left(\omega_h^{*2} - \omega_F^2\right) H_2^*}{|H_2^*| \sqrt{\left(\omega_h^{*2} - \omega_F^2\right)^2 + 4\zeta_h^{*2} \omega_h^{*2} \omega_F^2}} \tag{20}$$

For convenience, we rewrite Eq. (18) as follows

$$h_1 = h_{10} \sin\left(\omega_F t - \theta_1\right) \text{ with } \theta_1 = \theta - \frac{\pi}{2} \tag{21}$$

(iii) h_2 is the solution of forced vibration equation

$$\ddot{h} + 2\zeta_h^* \omega_h^* \dot{h} + \omega_h^{*2} h = \frac{\rho B^3}{2m} \omega_F^2 H_3^* \alpha_0 \sin \omega_F t \tag{22}$$

We find solution of Eq. (22) in the following form

$$h_2 = h_{20} \sin\left(\omega_F t - \theta_2\right) \tag{23}$$

with

$$h_{20} = \frac{\frac{\rho B^3}{2m} |H_3^*| \alpha_0 \omega_F^2}{\sqrt{\left(\omega_h^{*2} - \omega_F^2\right)^2 + 4\zeta_h^{*2} \omega_h^{*2} \omega_F^2}} \tag{24}$$

$$\sin\theta_2 = \frac{2\zeta_h^* \omega_h^* \omega_F H_3^*}{|H_3^*| \sqrt{\left(\omega_h^{*2} - \omega_F^2\right)^2 + 4\zeta_h^{*2} \omega_h^{*2} \omega_F^2}},$$

$$\cos\theta_2 = \frac{\left(\omega_h^{*2} - \omega_F^2\right) H_3^*}{|H_3^*| \sqrt{\left(\omega_h^{*2} - \omega_F^2\right)^2 + 4\zeta_h^{*2} \omega_h^{*2} \omega_F^2}} \tag{25}$$

Thus, the solution of heaving motion equation can be expressed as

$$h = h_{10} \sin\left(\omega_F t - \theta_1\right) + h_{20} \sin\left(\omega_F t - \theta_2\right)$$
$$\dot{h} = \dot{h}_1 + \dot{h}_2 = h_{10}\omega_F \cos\left(\omega_F t - \theta_1\right) + h_{20}\omega_F \cos\left(\omega_F t - \theta_2\right)$$

Expanding h, $\dot{h}$ and noting that $\sin\omega_F t = \frac{\alpha}{\alpha_0}$; $\cos\omega_F t = \frac{\dot{\alpha}}{\alpha_0 \omega}$, we obtain

$$
\begin{aligned}
h =\ & h_{10}\sin\left(\omega_F t - \theta_1\right) + h_{20}\sin\left(\omega_F t - \theta_2\right) \\
=\ & h_{10}\sin\omega_F t \cos\theta_1 - h_{10}\cos\omega_F t \sin\theta_1 + h_{20}\sin\omega_F t \cos\theta_2 - h_{20}\cos\omega_F t \sin\theta_2 \\
=\ & h_{10}\frac{\alpha}{\alpha_0}\cos\theta_1 - h_{10}\frac{\dot{\alpha}}{\alpha_0 \omega_F}\sin\theta_1 + h_{20}\frac{\alpha}{\alpha_0}\cos\theta_2 - h_{20}\frac{\dot{\alpha}}{\alpha_0 \omega_F}\sin\theta_2 \\
\dot{h} =\ & h_{10}\omega_F \cos\left(\omega_F t - \theta_1\right) + h_{20}\omega_F \cos\left(\omega_F t - \theta_2\right) \\
=\ & h_{10}\omega_F \cos\omega_F t \cos\theta_1 + h_{10}\omega_F \sin\omega_F t \sin\theta_1 + h_{20}\omega_F \cos\omega_F t \cos\theta_2 + h_{20}\omega_F \sin\omega_F t \sin\theta_2 \\
=\ & h_{10}\omega_F \frac{\dot{\alpha}}{\alpha_0 \omega_F}\cos\theta_1 + h_{10}\omega_F \frac{\alpha}{\alpha_0}\sin\theta_1 + h_{20}\omega_F \frac{\dot{\alpha}}{\alpha_0 \omega_F}\cos\theta_2 + h_{20}\omega_F \frac{\alpha}{\alpha_0}\sin\theta_2
\end{aligned}
\tag{26}
$$

Step 3: In torsional system, the torsional motion is generated by the heaving motion, which has a certain amplitude ratio and a certain phase difference, as free vibration

$$\ddot{\alpha} + 2\zeta_\alpha \omega_\alpha \dot{\alpha} + \omega_\alpha^2 \alpha = \frac{\rho B^3}{2I}\omega_F A_1^* \dot{h} + \frac{\rho B^3}{2I}\omega_F^2 A_4^* h + \frac{\rho B^4}{2I}\omega_F A_2^* \dot{\alpha} + \frac{\rho B^4}{2I}\omega_F^2 A_3^* \alpha \tag{27}$$

Expanding the heaving-oriented forced excitation in right-hand side of Eq. (27), we get

$$
\begin{aligned}
\frac{\rho B^3}{2I}\omega_F A_1^* \dot{h} + \frac{\rho B^3}{2I}\omega_F^2 A_4^* h = {} & \frac{\left(\frac{\rho B^3}{2I}\right)\left(\frac{\rho B^3}{2m}\right)\omega_F^2}{\sqrt{\left(\omega_h^{*2} - \omega_F^2\right)^2 + 4\zeta_h^{*2}\omega_h^{*2}\omega_F^2}} \cdot \Big[\left(\omega_F A_1^* |H_2^*|\cos\theta_1 + \omega_F A_1^* |H_3^*|\cos\theta_2\right. \\
& \left. - \omega_F |H_2^*| A_4^* \sin\theta_1 - \omega_F |H_3^*| A_4^* \sin\theta_2\right)\dot{\alpha} + \left(\omega_F^2 A_1^* |H_2^*|\sin\theta_1 + \omega_F^2 A_1^* |H_3^*|\sin\theta_2\right. \\
& \left. + \omega_F^2 |H_2^*| A_4^* \cos\theta_1 + \omega_F^2 |H_3^*| A_4^* \cos\theta_2\right)\alpha \Big]
\end{aligned}
\tag{28}
$$

For convenience, we use the following notations

$$\Omega_1 = \left(\frac{\rho B^4}{2I}\right); \Omega_2 = \frac{\left(\frac{\rho B^2}{2m}\right)\omega_F^2}{\sqrt{\left(\omega_h^{*2} - \omega_F^2\right)^2 + 4\zeta_h^{*2}\omega_h^{*2}\omega_F^2}} \cdot \frac{\left(\frac{\rho B^2}{2m}\right)\left(\frac{\omega_F}{\omega_h^*}\right)^2}{\sqrt{\left(1 - \left(\frac{\omega_F}{\omega_h^*}\right)^2\right)^2 + 4\zeta_h^{*2}\left(\frac{\omega_F}{\omega_h^*}\right)^2}} \quad (29)$$

Thus, we have

$$\begin{aligned}
\frac{\rho B^3}{2I}\omega_F A_1^* \dot{h} + \frac{\rho B^3}{2I}\omega_F^2 A_4^* h &= \Omega_1\Omega_2.[(\omega_F A_1^* |H_2^*| \cos\theta_1 + \omega_F A_1^* |H_3^*| \cos\theta_2 \\
&\quad - \omega_F |H_2^*| A_4^* \sin\theta_1 - \omega_F |H_3^*| A_4^* \sin\theta_2)\dot{\alpha} + (\omega_F^2 A_1^* |H_2^*| \sin\theta_1 + \omega_F^2 A_1^* |H_3^*| \sin\theta_2 \\
&\quad + \omega_F^2 |H_2^*| A_4^* \cos\theta_1 + \omega_F^2 |H_3^*| A_4^* \cos\theta_2)\alpha]
\end{aligned} \quad (30)$$

Substituting Eq. (30) into Eq. (27) yields

$$\begin{aligned}
\ddot{\alpha} + 2\zeta_\alpha\omega_\alpha\dot{\alpha} + \omega_\alpha^2\alpha &= \Omega_1\Omega_2[(\omega_F A_1^* |H_2^*| \cos\theta_1 + \omega_F A_1^* |H_3^*| \cos\theta_2 - \omega_F |H_2^*| A_4^* \sin\theta_1 \\
&\quad - \omega_F |H_3^*| A_4^* \sin\theta_2)\dot{\alpha} + (\omega_F^2 A_1^* |H_2^*| \sin\theta_1 + \omega_F^2 A_1^* |H_3^*| \sin\theta_2 + \omega_F^2 |H_2^*| A_4^* \cos\theta_1 \\
&\quad + \omega_F^2 |H_3^*| A_4^* \cos\theta_2)\alpha] + \frac{\rho B^4}{2I}\omega_F A_2^* \dot{\alpha} + \frac{\rho B^4}{2I}\omega_F^2 A_3^* \alpha
\end{aligned} \quad (31)$$

Eq. (31) can then be rewritten in the standard form as

$$\ddot{\alpha} + 2\zeta_F\omega_F\dot{\alpha} + \omega_F^2\alpha = 0 \quad (32)$$

where

$$\begin{aligned}
\omega_F &= [\omega_\alpha^2 - \Omega_1\omega_F^2 A_3^* - \Omega_1\Omega_2\omega_F^2(A_1^* |H_2^*| \sin\theta_1 + A_1^* |H_3^*| \sin\theta_2 \\
&\quad + |H_2^*| A_4^* \cos\theta_1 + |H_3^*| A_4^* \cos\theta_2)]^{1/2} = f(\omega_F)
\end{aligned} \quad (33)$$

$$\begin{aligned}
2\zeta_F &= 2\frac{\zeta_\alpha\omega_\alpha}{\omega_F} - \Omega_1 A_2^* - \Omega_1\Omega_2(A_1^* |H_2^*| \cos\theta_1 + A_1^* |H_3^*| \cos\theta_2 \\
&\quad - |H_2^*| A_4^* \sin\theta_1 - |H_3^*| A_4^* \sin\theta_2)
\end{aligned} \quad (34)$$

From Eq. (34) we have the formulation for Logarithmic decrement

$$\begin{aligned}
\delta_F &= 2\pi\zeta_F = 2\zeta_\alpha\omega_\alpha\frac{\pi}{\omega_F} - \pi\Omega_1 A_2^* - \pi\Omega_1\Omega_2(A_1^* |H_2^*| \cos\theta_1 + A_1^* |H_3^*| \cos\theta_2 \\
&\quad - |H_2^*| A_4^* \sin\theta_1 - |H_3^*| A_4^* \sin\theta_2)
\end{aligned} \quad (35)$$

Step 4: Finding the critical condition of flutter instability

Flutter instability occurs if only if Logarithmic decrement (Log. Dec) $\delta_F \leq 0$

$$\begin{aligned}
\delta_F &= 2\pi\zeta_F = 2\zeta_\alpha\omega_\alpha\frac{\pi}{\omega_F} - \pi\Omega_1 A_2^* - \pi\Omega_1\Omega_2(A_1^* |H_2^*| \cos\theta_1 + A_1^* |H_3^*| \cos\theta_2 \\
&\quad - |H_2^*| A_4^* \sin\theta_1 - |H_3^*| A_4^* \sin\theta_2) \leq 0.
\end{aligned}$$

Fig. 2 shows the flowchart for the step-by-step analysis (for torsional branch). According to the algorithm presented in this block diagram, a computer program was developed for calculating flutter vibration of bridges at the Department of Applied Mechanics of the Hanoi University of Science and Technology.
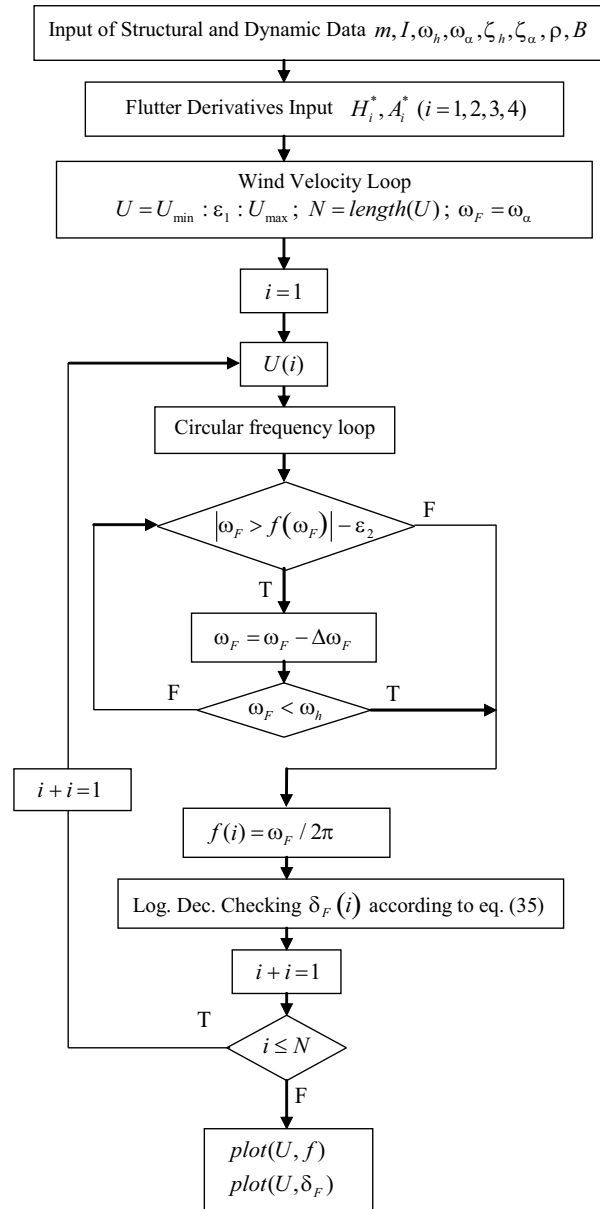
Fig. 2. Flowchart of step-by-step analysis (for torsional branch)

Stepwise procedure for torsional-branch analysis can be briefly presented hereinafter i) The torsional motion equation will be taken into first account in which torsional related coupled forces are considered as external oscillation, furthermore heaving motion solutions are found dependent on torsional vibration parameters; ii) Obtained heaving motion solutions will be transformed into torsional motion equation, then its damping ratio (or logarithmic decrement) will be determined in this torsional-branch; iii) Checking such a

damping ratio based on increment of reduced wind velocity to obtain a critical condition for torsional-branch flutter instability.

3. FLUTTER INSTABILITY ANALYSIS OF CAO LANH BRIDGE

Fig. 3 shows the side view of Cao Lanh cable-stayed Bridge, which was built in the Mekong Delta of Vietnam. The Cao Lanh Bridge represents the largest single Australian aid activity in mainland Southeast Asia and will help link people and markets in the Mekong Delta to the rest of Southeast Asia and beyond. The bridge will directly benefit five million people and is expected to deliver improved transport facilities to 170,000 daily road users within five years of completion.

Fig. 3. Side view of Cao Lanh cable-stayed bridge

Fig. 4. Free vibration analysis: Four fundamental natural mode shapes

Table 1. Flutter derivatives, angle of incidence 0^0, complete stage

U/fB	H_1^*	H_2^*	H_3^*	H_4^*	A_1^*	A_2^*	A_3^*	A_4^*
0.000	0.000	0.000	0.000	0.000	0.000	0.000	0.000	0.000
0.976	-0.019	-0.137	-0.061	-0.141	-0.108	-0.034	0.010	0.014
1.464	-0.318	-0.198	-0.163	-0.426	-0.219	-0.038	0.016	0.075
1.952	-0.642	-0.338	-0.381	-0.198	-0.178	-0.028	0.024	0.032
2.440	-0.402	-0.565	-0.432	-0.240	-0.367	-0.010	0.084	0.024
3.416	-1.118	-0.430	-0.533	-1.440	-0.468	-0.044	0.274	0.199
4.392	-2.426	-0.194	-1.968	-1.919	-0.513	-0.120	0.430	0.258
5.368	-3.730	0.288	-2.763	-2.115	-0.593	-0.182	0.584	0.312
6.344	-5.052	0.482	-4.562	-2.064	-0.680	-0.240	0.781	0.384
7.319	-6.344	0.566	-6.745	-1.856	-0.745	-0.314	1.015	0.444
8.295	-7.455	0.465	-9.142	-1.541	-0.804	-0.402	1.269	0.492
9.271	-8.406	0.186	-11.723	-1.053	-0.862	-0.519	1.531	0.541
10.247	-9.178	-0.194	-14.772	-0.706	-0.917	-0.638	1.810	0.537
11.223	-9.999	-0.652	-17.940	-0.403	-0.900	-0.781	2.103	0.591
12.199	-10.810	-1.119	-21.034	-0.312	-0.941	-0.909	2.388	0.635
13.175	-11.502	-1.770	-24.596	-0.201	-0.959	-1.055	2.703	0.661
14.639	-12.765	-2.609	-30.351	-0.311	-1.013	-1.291	3.209	0.675
16.103	-13.851	-3.423	-36.515	-0.288	-1.069	-1.514	3.752	0.663
17.567	-15.087	-5.136	-43.175	-0.324	-1.117	-1.768	4.301	0.635
19.031	-16.534	-6.324	-50.321	-0.054	-1.209	-2.026	4.904	0.586
20.494	-17.428	-7.789	-58.192	-0.033	-1.431	-2.243	5.612	0.443

Numerical calculating of the Cao Lanh cable-stayed bridge for the flutter analysis is presented in this section. The following geometry and material data of the bridge deck have been used for the numerical calculation:

$m = 52039 \, \text{kg/m}, I = 3968530 \, \text{kgm}^2/\text{m}, f_h = 0.296 \, \text{Hz}, f_\alpha = 0.620 \, \text{Hz}, \zeta_h = 0.008,$ $\zeta_\alpha = 0.008, B = 27.5 \, \text{m}, \rho = 1.25 \, \text{kg/m}^3$.

Tab. 1 shows the experimental results of Flutter derivatives [10]. Some calculating results are displayed in Figs. 4-7.

Fig. 4 shows some natural mode shapes of the Cao Lanh cable-stayed bridge [10]. From the data given in Table 1 we can calculate diagrams of flutter derivatives A_i^*, H_i^* ($i = 1, 2, 3, 4$) as shown in Fig. 5. In Figs. 6 and 7 are diagrams $U - f$ and $U - \delta_F$.

The calculated flutter speed of Cao Lanh Bridge is upper 100 m/s. Ref. [10] gives the flutter speed of the bridge using a section model upper 98.3 m/s, which is in agreement with the calculated result.
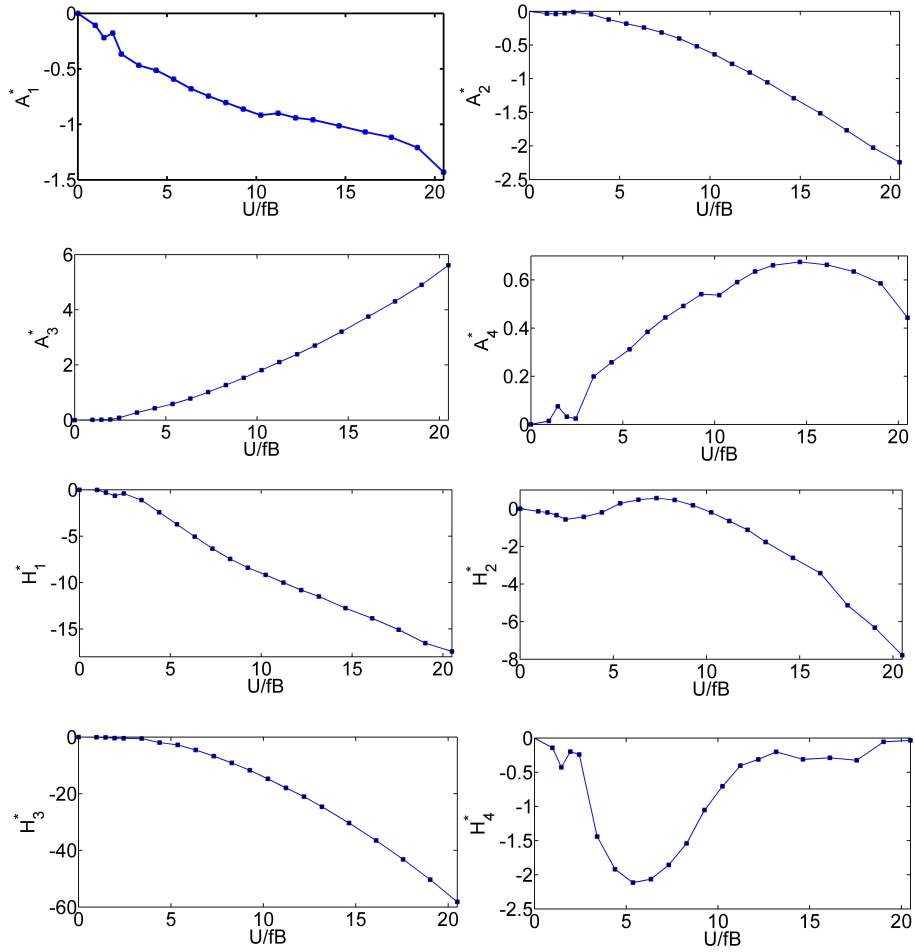
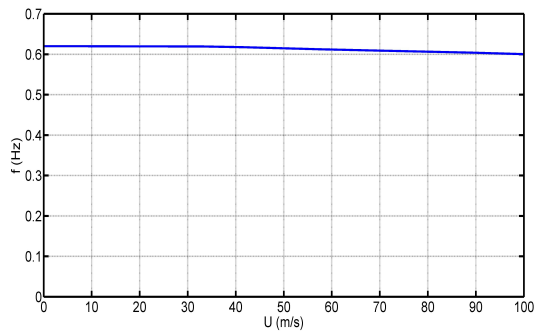*Fig. 5.* Diagrams of flutter derivatives A_i^*, H_i^* ($i = 1, 2, 3, 4$)
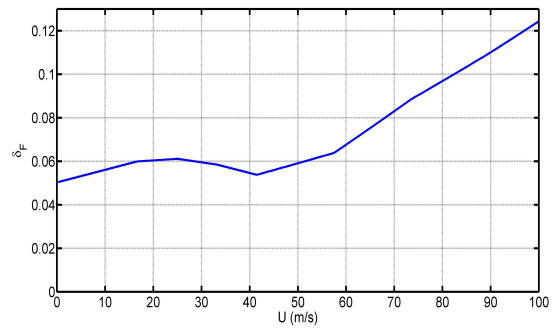

Fig. 6. $U - f$ diagram

Fig. 7. $U - \delta_F$ diagram

4. CONCLUSION

The step-by-step method is based on the serial solving technique of two heaving-torsional motion equations, solutions of the former equation are used to determine coupled aerodynamic forces subjected to the later equation. From transformation process, there is torsional-branch or heaving-branch step-by-step method. Because torsional-branch instability dominates in almost cases, the torsional-branch step-by-step analysis will be favorable to be much more applicable in comparison with heaving-branch one. The step-by-step method is also favorable to deal with the complex eigenvalue method's limitation. In this paper, a revised step-by-step analysis method is proposed and a calculating program using MATLAB is developed. The step-by-step method is applied for calculating the flutter instability of the Cao Lanh cable-stayed Bridge, which was built in Mekong Delta of Vietnam. The calculation results obtained are consistent with experimental results.

ACKNOWLEDGMENT

REFERENCES

[1] R. H. Scanlan and E. Simiu. *Wind effects on structures*. Wiley, (1996).

[2] U. Starossek. *Brueckendynamik: Winderregte Schwingungen von Seilbruecken*. Vieweg, Braunschweig/Wiesbaden, (1992).

[3] J. Banerjee. A simplified method for the free vibration and flutter analysis of bridge decks. *Journal of sound and vibration*, **260**(5), (2003), pp. 829–845.

[4] L. T. Hoa. *Flutter stability analysis: Theory and Example*. www.uet.vnu.edu.vn/thle, (2004).

[5] M. Iwamoto and Y. Fujino. Identification of flutter derivatives of bridge deck from free vibration data. *Journal of Wind Engineering and Industrial Aerodynamics*, **54**, (1995), pp. 55–63.

[6] M. Matsumoto, K. Kobayashi, Y. Niihara, H. Shirato, and H. Hamasaki. Flutter mechanism and its stabilization of bluff bodies. In *Proceedings of the Ninth Conference on Wind Engineering*, Vol. 2, pp. 827–838, (1995).

[7] M. Matsumoto, K. Mizuno, K. Okubo, Y. Ito, and H. Matsumiya. Flutter instability and recent development in stabilization of structures. *Journal of Wind Engineering and Industrial Aerodynamics*, **95**(9), (2007), pp. 888–907.

[8] M. Matsumoto, H. Matsumiya, S. Fujiwara, and Y. Ito. New consideration on flutter properties based on step-by-step analysis. *Journal of Wind Engineering and Industrial Aerodynamics*, **98**(8), (2010), pp. 429–437.

[9] D. J. Inman and R. C. Singh. *Engineering vibration*. Prentice Hall New Jersey, (2001).

[10] B. Barwick. *Cao Lanh bridge design report*, Vol. I, II. (2012).

CONTENTS

Pages